Contents lists available at YXpublications

International Journal of Applied Mathematics in Control Engineering

Journal homepage: http://www.ijamce.com

Numerical Simulation of Heat Transfer in High Temperature Liquid Slag Breaking and Granulation Process

Jincai Chang[a,*], Yafei Zhu[a], Qiuling Pan[a], Xing Xin[a]

[a] *School of Science, North China University of Science and Technology, Hebei Tangshan, 063009, China*

ARTICLE INFO

Article history:
Received 24 November 2018
Accepted 30 January 2019
Available online 30 June 2019

Keywords:
Numerical simulation
Granulation
VOF interface tracking method
Flow field
Fluid heat transfer
Differential equation numerical solution
Multi physical field coupling
SIMPLE algorithm

ABSTRACT

High temperature liquid slag is a by-product in metal smelting process. In the actual metal smelting project, the temperature is up to 1000 degrees, so the metallurgy workers do not know exactly the variation of the physical field in crushing and granulation procedure of liquid thermal liquid slag. And for that reason, the utilization and treatment technology of thermal slag liquid has not been mature so far. At the same time, because of this reason, the utilization and treatment technology of high temperature liquid slag is not yet mature. In this paper, the classical physical equation and the SIMPLE algorithm, and the VOF interface tracking method are combined by studying heat transfer theory to optimize the calculation method and establish the mathematical model. Finally, using the numerical simulation software COMSOL of multi-physical coupled-field，the granular procedure of high-temperature liquid slag is simulated，and the comparatively accurate result is obtained. According to the research work of this paper, the physical mechanism of the high temperature liquid slag in the process of crushing and granulation is summarized, and the research ideas in the related fields are provided, which have some enlightening and practical value for the related research work.

1. Introduction

High temperature liquid slag is a by-product of metal smelting production, which accounts for about 15% of steel production. The annual output of steel-making slag in the world amounts to tens of millions of tons. If these high-temperature liquid slags are being underutilized, they will have a great impact on the environment, and the high-temperature liquid slag of the converter contains a large amount of sensible heat. If these high-temperature liquid slags are naturally cooled in the slag field for a long time, it will not only pollute the environment but also causes great waste of energy [1]. Therefore, in order to meet the requirements of modern industries the comprehensive utilization of liquid high temperature liquid slag must be considered [2]. At present, there is no more reasonable way for the treatment of high temperature liquid slag in China, which can not only make good use of the treated slag but also not pollute the environment and recover high temperature liquid residue. It has become an important task for metallurgical workers to develop a new process and new methodology for liquid high temperature liquid slag treatment that can be in line with the “comprehensively deepen supply-side structural reform” principle.

* Corresponding author.
E-mail addresses: jincai@ncst.edu.cn (J. Chang)

Wind air-granulated method. The liquid high-temperature liquid slag is poured from the slag ladle into the slag tank, and a granulation metallurgical slags blower is arranged under the slags pout. When the high-temperature liquid slag flows out from the end of the slag tank, it will be divided by the high-speed air flow jetted from the blower [3]. The air-granulated method has features such as simple technology, little space, low invest, low maintenance, safety and high efficiency, particle with stable performance and thorough granulation. The main disadvantages of this technology are as follows: high temperature liquid slag must be liquid high temperature liquid slag. In order to control the flow rate of slag, high temperature liquid slag must pass through the intermediate tank. Most of the air quenching gas utilizes air. Due to oxidation, the elemental iron in the granulated high temperature liquid slag is easily oxidized and cannot be recovered because of oxidation [4].

Traditional numerical research methods include three kinds: theoretical research methods, experimental methods, and numerical methods. Among them, numerical methods are one of the fastest-growing methods in modern analytical methods. The advantages of the theoretical research method are low cost, good results and the factors are clearly expressed, but the method is limited to very simple problems. Although the experimental method is reliable but

limited by the model, the cost is high and the period is long. The numerical method is low in cost and wide in application but is subject to calculation resource and model .Therefore, thesis has its necessity and practical significance.

2. The proof of COMSOL and PDE model

2.1 Introduction to COMSOL

COMSOL is multidiscipline coupled-field simulation software based on finite element method. The software is mainly composed of "model developer" and "app developer".

Guiding by the model tree, the "model developer" is composed of tools and components for defining and building model. In addition, the developer can also change the solution approach, analysis the model results and create the result report. The design of the model tree can reflect the design principle and data structure of the underlying layer. The state of the storage model includes the following settings: geometry selection, meshing, physical field selection, boundary condition setting, research model, post-processing, and simulation of squared results [5].

The "APP Developer" includes menu bars, ribbons and two important editors--"form editor" and the "method editor". The Form Editor can add apps, such as windows and buttons, to the models required by the user group interface. The Method Editor is a programming environment that allows you to modify the original data objects and models to accommodate new requirements [6].

2.2 The proof of COMSOL

The mathematical software is based on finite element, and the solution process can be represented by Figure 2-1.

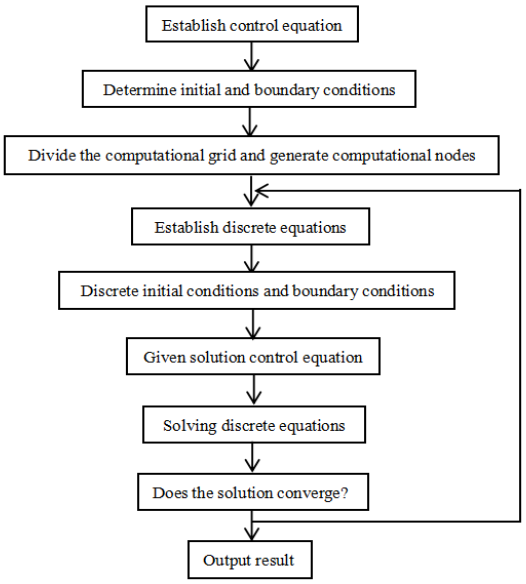

Fig.2.1 Solving process of COMSOL internal equation

2.3 Finite Element Method and PDE Mode in COMSOL

2.3.1 Finite element method in COMSOL

As finite element simulation software, COMSOL provides a PDE mode based on mathematical equations to solve practical problems. This model can simulate the numerical simulation analysis of multi-physical field coupling. The model is composed of finite element method partial differential equations. Study high temperature liquid slag flow and solidification. This model used four physical field interfaces in COMSOL, namely laminar flow model (spf), fluid model (ht), dilute material transfer model (chds) and point weak partial differential equation model (wp) ，which is a multi-physics numerical simulation model of coupled complex fields [7].

In the COMSOL math operation, PDE mode, we can input the appropriate governing equations and initial boundary conditions according to the problem studied.That is to deduce and set the step of "mathematical modeling" in Figure 2.2, in which three ways of input governing equations are provided [8].

The first is the"coefficient type", which provides a generic equation template:

$$e_\alpha \frac{\partial u^2}{\partial t^2} + d_a \frac{\partial u}{\partial t} + \nabla.(-c\nabla u - \alpha_u + \gamma) + au + \beta.\nabla u = f \quad (1)$$

where: u is the field variable; t is the time; ∇ is the Hamiltonian; the other is the parameter to be input, and the control equation that conforms to the actual problem can be obtained by setting the parameter to be input in equation (1) [9].

The second type is "generic type", and the equation template provided by this type is:

$$e_a \frac{\partial^2 u}{\partial^2 t} + d_a \frac{\partial u}{\partial t} + \nabla.\Gamma = F \quad (2)$$

where: Γ is a generalized flux. This type also achieves the required governing equation by setting the input parameters.

2.3.2 PDE mode in COMSOL

The equations established by "coefficient type" and "general use type" are automatically converted into "weak form" during the solution process, that is, the "variation principle" step in Figure 2-2 is completed by the software built-in program. The governing equations for some common problems can be set by two methods, such as heat conduction equation, laminar flow equation, etc. [10]. However, the mathematical description of some problems is difficult to express in two ways, such as high temperature liquid slag flow and solidification model.

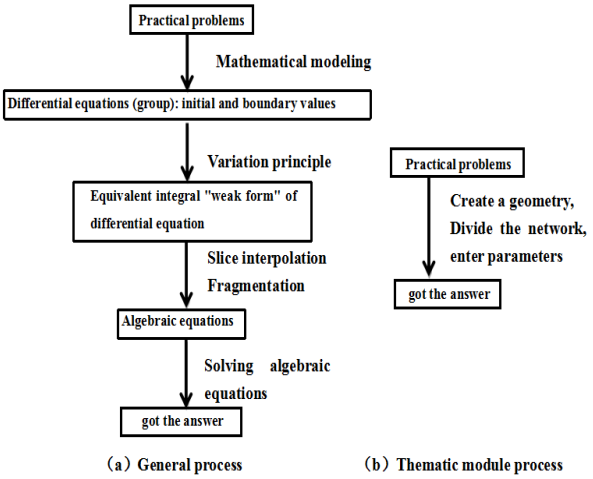

Fig. 2.2 Flow chart of finite element method

In addition, the third method of establishing a mathematical model, namely "weak form", is to obtain a mathematical expression of a wider range of problems by setting the equivalent integral equation. The "weak form" is

$$\int_{\Omega} \omega_s dA + \int_{\partial\Omega} \omega_b ds = 0 \tag{3}$$

where: ω_s and ω_b are the weak terms on the solution domain Ω and the boundary Ω respectively. The "weak form" equation is essentially to manually complete the two parts of the "mathematical modeling" and "Variation principle" in Figure 2.2. It is more flexible to directly input the equivalent weak form of differential equation into the software [11].

3. Study on high temperature liquid slag crushing and granulation process

The surface behavior of high temperature liquid slag is the key to studying the granulation process. At present, we can't get the behavioral characteristics of the granulation process from the actual experiment. Therefore, this paper utilize the coupled field numerical analysis tool COMSOL on the numerical simulation of the granulation process to make up the lack of experiment, and provide innovative ideas for the same type of numerical simulation.

In this chapter, the SIMPLE algorithm is used to simulate the process of high temperature liquid slag gas quenching and granulation, so as to analyze and discuss the mechanism of high temperature liquid slag crushing and granulation.

3.1 Basic control equation for granulation

In the process of crushing and granulating high-temperature liquid slag, any kind of chemical reaction is involved, and the total mass before and after the reaction does not change [12]. The quality of matter does not increase or decrease, it can only be transformed from one form to another. Mass conservation equation:

$$\frac{\partial u}{\partial t} + \nabla.(\rho\vec{u}) = 0 \tag{4}$$

The momentum conservation equation is one of the most important and common conservation principles in nature, which applies to both macroscopic and microscopic particles [13]. And it is not only applies to the low-speed and high-speed moving objects, but to the conservative and non-conservative systems. The equation is:

$$\frac{\partial}{\partial t}(\rho\vec{u}) + \nabla.(\rho\vec{u}) = \nabla.\mu(\nabla\vec{u}) - \nabla p + \rho g + \sigma k \delta_s \vec{n} \tag{5}$$

The total energy change of all materials during the crushing and granulation of high-temperature liquid slag can only be equal to the amount of the energy passed into or out of the system. The total energy is the combination of the mechanical energy, thermal energy and any internal energy of the system [14]. The energy conservation equation is:

$$\frac{\partial}{\partial t}(\rho CT) + \nabla.(\rho C_p T\vec{u}) = \nabla.\lambda(\nabla T) + \varphi \tag{6}$$

The above three equations: u is the speed, ρ is the density, μ is the dynamic viscosity, p is the pressure, σ is the surface tension, k is the surface free rate, δ_s is the Dirac function on the interface s, and n is the free interface on unit law vector, λ is the thermal conductivity, T is the temperature, and ϕ is the latent heat absorbed and released when the interface undergoes a phase change.

A continuous surface tension model proposed by Brackbill J.U. [15] was selected to simulate evaporation and condensation at the water-steam interface. The mass exchange was:

$$mh_{fg} = (\bar{q}_l - \bar{q}_v)\bar{n} + \psi = (\lambda_l \frac{\partial T}{\partial n}\Big|_l - \lambda_v \frac{\partial T}{\partial n}\Big|_v) + \psi \tag{8}$$

In the above formula, $\bar{q}$ is the heat exchange between water and steam, and ψ is the heat transferred.

In this paper, the portion of water, steam, and high temperature liquid slag in the grid control volume is set to C_i, and their transport equations are:

$$\frac{\partial C_i}{\partial t} + \frac{\partial C_i u}{\partial x} + \frac{\partial C_i u}{\partial y} + \frac{\partial C_i u}{\partial z} = \Gamma_i \tag{8}$$

Γ_i phase change from three media causes a change in volume fraction.

The physical properties of water, steam and high temperature liquid slag are now expressed as follows:

$$\begin{aligned} \rho &= \sum C_i \rho_i \\ \mu &= \sum C_i \mu_i \\ \lambda &= \sum C_i \lambda_i \\ C_p &= \sum C_i C_{pi} \end{aligned} \tag{9}$$

3.2 Numerical calculation method

3.2.1SIMPLE algorithm

Since the solution process of high temperature liquid slag is to solute a coupled field, the current methods are coupled solution method and separate solution method. Because the coupling method is computationally inefficient and requires high computational software. The separate pressure correction algorithm is the most widely used method in multi-physical field coupling calculation at present, and SIMPLE can realize the pressure correction algorithm.

The idea of the SIMPLE algorithm is to solve the algebraic equations in turn when the pressure field is given. Thus, a momentum equation that satisfies the local continuity is obtained. But it is not necessarily globally continuous and the pressure equation must be corrected. Substituting the pressure and velocity in the discrete momentum equation into the continuity equation to correct the pressure equation [16]. Then the velocity equation is used to improve the velocity, and the new velocity is substituted into the momentum discrete equation until to obtain a stable convergence solution.

Correcting the velocity and pressure of equation. We set the initial pressure and the three-dimensional velocity field be p_0, u_0, v_0, w_0 respectively. Subtracting the original pressure from the improvement value and the corrected pressure P' is obtained. The relationship is as follows:

$$\begin{aligned} u &= u_0 + u' \\ v &= v_0 + v' \\ w &= w_0 + w' \\ p &= p_0 + p' \end{aligned} \tag{10}$$

The resulting momentum equation is:

$$A_p u_p = \sum_{M-E,W,N,S,T,B} AMuM + S_l^u - \frac{\partial p}{\partial x}\Big|_p \Delta V_x$$

$$A_p u_p = \sum_{M-E,W,N,S,T,B} AMuM + S_l^v - \left.\frac{\partial p}{\partial_y}\right|_p \Delta V_y \qquad (11)$$

$$A_p u_p = \sum_{M-E,W,N,S,T,B} AMuM + S_l^w - \left.\frac{\partial p}{\partial z}\right|_p \Delta V_z$$

In the above formula, S_l^u, S_l^v, S_l^w is the sum of the other terms of the discrete momentum equation except pressure. According to the correction relationship of equation (10), the velocity of the three-dimensional coordinates can be obtained.

The conservation equation is solved iteratively by SIMPLE algorithm, and then the convergence of the test results of the mass conservation equation is substituted. The specific solution steps are shown in Figure 3.1:

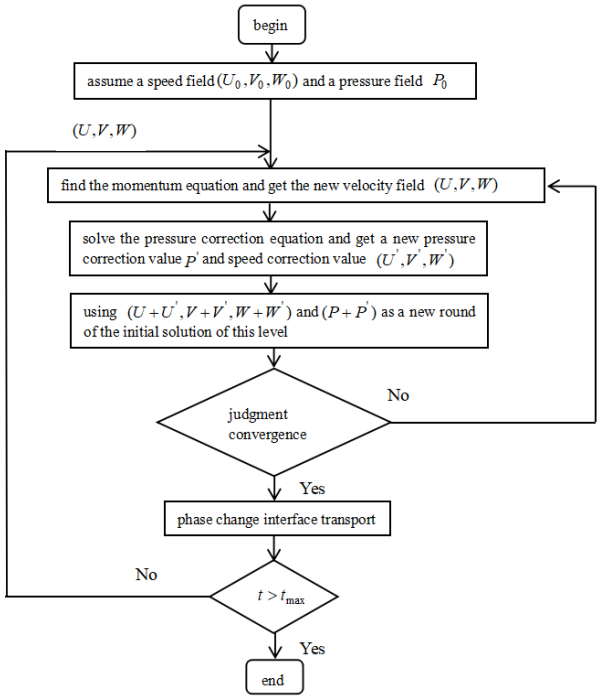

Fig.3.1 Iterative solution procedure of SIMPLE algorithm

3.2.2 Interface Tracking Algorithm

In this paper, the VOF method is used to study the interface tracking algorithm. This algorithm is similar to the 0-1 algorithm in fuzzy mathematics. Taking the two fluids of vapor and liquid as an example, if C represents a volume fraction, $C=0$ represents a liquid phase, then $C=1$ represents a gas phase, and $0<C<1$ represents a gas-liquid two-phase mixed control body [17]. Since C changes over time, a fixed time step is required to calculate the amount of volume that each control surface passes through. The geometry of the fluid is controlled by the reconstruction of the surface. Solve C by transport equation:

$$C_i + \nabla.(\bar{V}C) = S \qquad (12)$$

In the above formula, C is the volume fraction, V is the velocity vector, and S is the source phase.

In this algorithm, a multi-phase control body interface is represented by a straight line. Take the grid split example, as shown in Figure 3.2.

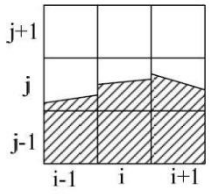

Fig.3-2 Two-dimensional uniform grid interface normal vector

The polygon enclosed by the oblique line in the above figure represents the volume share of the fluid. The physical meaning of the normal direction of the interface is again the gradient direction of the volume fraction. Try to find the angle between the line and the x axis as β and unitize β to α .

$$\beta = \tan^{-1}(\frac{-n^x}{n^y}), \alpha = \tan^{-1}(\frac{\delta x}{\delta y}\tan\beta)(\pi/2 \le \alpha \le \pi) \qquad (13)$$

Based on the volume share function and the straight normal vector, the line equation can be determined. As shown in Figure 3-3, the distance from A to the interface is:

$$l = \min d(EH, A) \qquad (14)$$

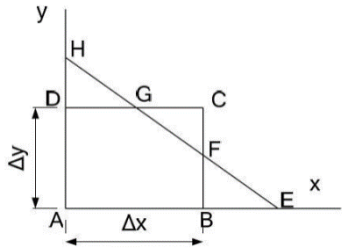

Fig.3.3 Interface reconstruction of linear equation

In Figure 3-3, ABFGD is the target area of the fluid, and the area can be expressed as:

$$S_{ABFGD} = \frac{l^2}{2n_1 n_2}\begin{bmatrix} 1 - H(l - n_1\Delta x)(\frac{l - n_1\Delta x}{l})^2 \\ -H(l - n_1\Delta y)(\frac{l - n_2\Delta y}{l}) \end{bmatrix} \qquad (15)$$

In the above formula, H is the Heaviside more-order function. It can be seen that if l is obtained, then α can be used to uniquely determine the interface position.

3.2.3 Multi-physical field coupling *processing method*

The VOF method is difficult to achieve when a multi-phase coupled physics field occurs. As shown in Figures 3.4, it is a hybrid control body comprising a liquid phase and a gas phase. It is assumed that the right surface of the control body can be displaced or deformed, and the liquid phase is continuously evaporated to remove water vapor, so that the right surface of the control body is compressed by water vapor, thereby having a horizontal rightward velocity. The vaporized water vapor is tracked by the VOF method, and after a period of time, the area of the shaded portion appears as shown [18]. In reality, the liquid phase of the control body is zero, and the water is emitted by the water vapor. Because of the evaporation relationship, the volume of the liquid phase should be slightly reduced.

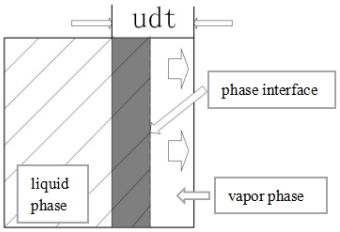

Fig.3.4 Mixed control body of liquid phase and vapor phase

In reality, it is difficult to calculate the variation of the volume due to the uncertainty of the straight line and the velocity field of the reconstructed interface. In this paper, the gas-liquid mixture is distributed to the nearest all gas phase. Calculating the dispersion of velocity field on the control volume is zero by using the approximation method, in which the velocity field is solved by continuity equation. Therefore, the VOF method can control the control volume of the multi-phase coupling by approximation [19]. Because of the surface tracking algorithm, the study only needs to calculate the variation of the liquid phase, and the result can be calculated by the conservation equation.

3.2.4 Continuous surface tension model

Surface tension is due to the imbalance of molecular gravity. In general, the forces of different molecules are different. If the resultant force of the molecule is not zero and cannot be in equilibrium, it will cause the surface of the liquid to automatically scale. The force generated by this phenomenon is the surface tension. The magnitude of the surface tension is related to the temperature of the medium and the nature of the multi-phase coupling. Because tension exists only on the surface of the liquid, all variables in the numerical calculations exist on the boundary of the mesh [20]. In this paper, the surface tension model CFS is used to study it. The unit area force equivalent to the tension in the momentum equation is calculated as follows:

$$F_{sa}(x_s) = \sigma k(x_s)\vec{n}(x_s) \tag{16}$$

In the above formula, x is a spatial position vector, σ is a tension coefficient, k is an interface curvature, and n is a unit normal vector pointing in the fluid. In the actual calculation, we use the integral method to get a smooth surface as much as possible, and integrate the unit area force:

$$\lim_{h\to 0}\int_{\Delta v} F_{sv}(x)d^3x = \int_{\Delta A} F_{sa}(x_s)dA \tag{17}$$

Through the integral calculation, you can get:

$$Fsv(x) = \sigma k(x)\frac{\nabla\vec{c}(x)}{[c]} \tag{18}$$

also because:

$$k = -(\nabla.\vec{n})$$
$$\vec{n}(x) = \frac{\nabla\vec{c}(x)}{|\nabla\vec{c}(x)|} \tag{19}$$

In addition to this, the normal vector is expressed as follows:

$$n(x) = \nabla\vec{c}(x) \tag{20}$$

Combining equation (20), we can calculate that the curvature k is:

$$k = \frac{1}{|n|}[(\frac{n}{|n|}.\nabla)|n| - (\nabla.n)] \tag{21}$$

4. Mathematical model establishment and numerical simulation based on COMSOL

4.1 Control equations in COMSOL and the establishment of mathematical models

The Cahn-Hilliard convection equation is a conceptual model that minimizes the energy of time [21]. It enhances the protection of the field by approximating the interface diffusion flux proportional to the chemical potential gradient. This equation simulates the generation, evolution, and dissolution of the interface:

$$\frac{\partial\phi}{\partial t} + u.\nabla\phi = \nabla.(M\nabla G) \tag{22}$$

where ϕ is the concentration fraction of the two components, which is referred to as the order parameter. It has different constant values throughout the phase and the invariant values vary rapidly between interfaces. M is a diffusion coefficient called fluidity, which governs the diffusion-dependent time scale of the interface, and G is the chemical potential of the system. Fluidity can be expressed as $M = M\varepsilon^2$, where M_c is the interface thickness dimension that controls the mobility of the diffusion and time stability characteristics. The chemical potential is obtained from the total energy equation $G = \lambda[\phi(\phi^2-1)/\varepsilon^2 - \nabla^2\phi]$, λ represents the mixed energy density. Equation (22) shows that the evolution of ϕ over time depends on convective transport due to the divergence velocity and diffusion of the chemical potential gradient transport.

In order to simulate the high temperature liquid slag flow and solidification problems, equation (22) is combined with the incompressible Navier-Stokes and continuity equations. The surface tension and variable physical properties are as follows:

$$\nabla.u = 0 \tag{23}$$

$$\rho\frac{\partial u}{\partial t} + \rho u.\nabla u = -\nabla p + \nabla[\mu(\nabla u + \nabla u^T)] + F_{st} \tag{24}$$

Equation (23) represents the constraint of the incompressibility of the fluid. Equation (24) Navier-Stokes equations describe fluid flow [22].In these expressions ρ and η are fluid density and viscosity, respectively. The reverse permeability of the porous medium α is assumed to be approximately effective for the actual porous medium. The state variables are fluid pressure P and velocity field u

In addition, the governing equation for steady-state convective diffusion heat transfer is:

$$\rho C(u.\nabla T) = \nabla.(k\nabla T) + Q \tag{25}$$

where C is the heat capacity and k is the thermal conductivity of the fluid.

In the actual problem，In order to achieve optimal heat transfer and fluid flow, It is proposed to use the dual objective function A_2 here. Specifically, the target is specified to minimize the average temperature and total fluid power consumed in the system.

$$A_2 = w_1 B + w_2 C \tag{26}$$

$$B = \int_{\Omega}\{k\gamma(\nabla T)^2 + \rho C[T(u.\nabla T)]\}d\Omega \tag{27}$$

$$C=\int_{\Omega}\left[\frac{1}{2}\eta\sum_{i.j}\left(\frac{\partial u_i}{\partial x_j}+\frac{\partial u_j}{\partial x_i}\right)^2+\sum_i\alpha\gamma u_i{}^2\right]d\Omega \quad (28)$$

The above equation (26) is implemented as a global expression. In this expression, B is proportional to the average temperature of the design region of constant heat generation Q, and C is related to the total flow power in the fluid system.

In terms of equations w_1 and w_2 are the portions of the thermal fluid of the objective function of the weighted value scale .Finding these values helps to converge and modifies the final best topology by affecting the advantages of one physical process relative to another. For the sake of simplicity, these weight values are manually selected.

In order to determine the optimal steady-state fluid flow and channel layout, the thermal conductivity and the reverse permeability coefficient of the porous medium were interpolated using the convex interpolation format [23]. These effective properties (ie, k and α) are interpolated by the main design parameters γ varying from 0 (non-conductive solids) to 1 (conductive liquids).

The surface force of the object is calculated by deriving the total free energy in the space coordinate system. The results are as follows:

$$F_{st}=G\nabla\phi \quad (29)$$

It is considered that the surface tension is an intrinsic property corresponding to the excess free energy density of the interface region. The metal surface tension coefficient is equal to the integral of the free energy density of the entire interface, which is the case of $\sigma=2\sqrt{2}\lambda/(3\varepsilon)$ in the planar interface.

In order to include the effects of temperature in the model, the thermal equation must also be coupled to the interface equation (22) , the momentum equation (26) and the continuity equation (27). The heat equation for fluids, including convection and conduction heat transfer, is obtained as follows:

$$\rho C_p\frac{\partial T}{\partial t}+\rho C_p u.\nabla T=\nabla.(k\nabla T) \quad (30)$$

where T is the absolute temperature, C_p is the specific heat capacity, and k is the thermal conductivity. C_p and k are defined as a function of the order parameter to obtain a constant value in the bulk phase and smoothly change through the interface.

The built-in laminar two-phase flow is numerically simulated with the heat transfer module COMSOL.

4.2 Boundary conditions of COMDE-based PDE model

4.2.1 Laminar Flow Model

Laminar flow is a flow state of fluid that flows as a laminate. The fluid appears as laminar flow when flowing at low speed in the tube. Since the flow of high temperature liquid slag conforms to the motion characteristics of laminar flow [24], we establish a laminar flow model.

According to the mass conservation governing equation, we can get the following governing equation:

$$\frac{\partial\rho}{\partial t}+\nabla.(\rho u)=0 \quad (31)$$

$$K-(K.n)n=0$$

$$K=\left[\mu\left(\nabla u+(\nabla u)^T\right)-\frac{2}{3}\mu(\nabla.u)I\right]n \quad (32)$$

Volume force：

$$F(x,y)=(-Sx*Hphi+Fx,-Sy*Hphi+rho*gy+Fy) \quad (33)$$

The constraints and letters in the laminar flow model are shown in Table 4.1 below.

Table4-1 The property or value of a constraint for a laminar model

constraint name	attribute or value	constraint name	attribute or value
label	Laminar Flow	turbulence model type	null
reference pressure level	$p_{ref}=1[atm]$	material damping coefficient	$\mu=eta$
dynamic viscosity equation	$\mu=0$	boundary conditions	no slip
velocity field	$u(x,y,z)=(0,0,0)$	pressure constraint	$p_0=0$
symmetric hypothesis equation	$u.n=0$	compressibility	compressible（Ma<0.3)

4.2.2 Heat Transfer in Fluids Model

Equation:

$$d_z\rho C_p\frac{\partial T}{\partial t}+d_z\rho C_p u.\nabla T=\nabla.(d_z k\nabla T)+d_z Q+Q_{vd}+Q_p+Q_{oop} \quad (34)$$

The constraints and letters in the fluid heat transfer model are shown in Table 4.2 below.

Table4.2 Fluid heat transfer model is the property or value of the constraint name

constraint name	attribute or value	constraint name	attribute or value
thickness	$d_z=1$	absolute pressure	$p_A=1[atm]$
thermal conductivity	$K=k$	density	$\rho=rho$
atmospheric pressure	$C_p=cpT$	specific heat rate	$\gamma=1$
boundary selection	$-n.(-d_z k\nabla T)=0$	temperature	$T=T_i$
assumed equation	$T=T_0$	temperature	$T_0=T_c$

4.2.3 Transport of Diluted Species model

Control equation:

$$\frac{\partial c_i}{\partial t}+\nabla.(-D_i\nabla c_i)+u.\nabla c_i=R_i \quad (35)$$

$$N_i=-D_i\nabla c_i+uc_i \quad (36)$$

The constraints and letters in the dilute material transfer mo

del are shown in Table 4.3 below.

Table4.3 A property or value that constrains the name of a dilute material transfer model

constraint name	attribute or value	constraint name	attribute or value
label	Transport of Diluted Species	Transfer mechanism	convection
number of substances	1	concentration	phi
velocity field	u	diffusion coefficient	D_{phi}
concentration	$phi = phi0$	reaction speed	$R_{phi} = lamb * smdelta$
Assumed equation	$u.n = 0$	compressibility	compressible flow （Ma<0.3)

k	$kg + (k1 - kg) * Hphi$	int $phi0$	int $top1(Hphi0)$
Fs	$1 - lambd$	A	$-C*(1-lambd)\text{^}2 /(lambd\text{^}3+q)$
Sx	$-A*u$	Sy	$-A*u$
cpH	$L* fldc2hs(T-Tm,e)$	cpT	$cp + cpH$
$Hphi0$	$(1+\tanh(-phi0/n))/2$	$smdelta$	$n2/sqrt(pi) *\exp(-n2\text{^}2* phi\text{^}2)$
$lamb$	int $top2(lam)$	Fx	$sigma*kappa*smdelta * phix$
Fy	$sigma*kappa*smedlta * phiy$	int phi	int $top1(Hphi)$

4.2.4 Point weak partial differential equation (PDE) model

Label: PDE

Name: wp

Assume the equation: $0 = \sum_{pi} weak_i$

Weak expression:

$$weak = test(lam) * (\text{int } phi - \text{int } phi0) \tag{37}$$

Initial value: $lam = 0$

$$\frac{\partial lam}{\partial t} = 0$$

4.3 COMSOL high temperature liquid slag crushing and granulating simulation

4.3.1 Model Properties and Expressions

Set the entire model properties in the four physical models of COMSOL Multiphysics, and enter the corresponding variable name and value or expression (Table 4-4).

Table4-4 Variable name (corresponding mathematical symbol) and its expression

variable name	value or expression	variable name	value or expression
x_0	0	y_0	0
r	0.5	$rhog$	1
$rhol$	10	$etal$	1
gy	-10	n	0.02
T_i	1	T_c	-0.2
e	0.1	cp	1
$phi0$	$sqrt((x-x0)\text{^}2 +(y-y0)\text{^}2)-r$	$Hphi$	$(1+\tanh(-phi/n))/2$
rho	$rhog + (rho1 - rhog) * Hphi$	eta	$etag + (eta1 - etag) * Hphi$

4.3.2 Simulation simulation diagram display

The simulation of the change process of the free interface under the pressure pulse is shown in Figure 4-1:

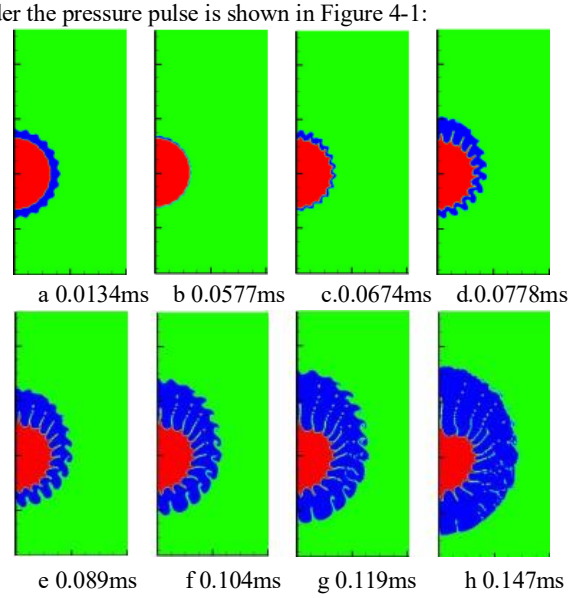

a 0.0134ms b 0.0577ms c.0.0674ms d.0.0778ms

e 0.089ms f 0.104ms g 0.119ms h 0.147ms

Fig. 4.1 The change process of the free interface of high temperature liquid slag

Pictures a and b indicate that the pressure is transmitted from the bottom up to the position of the high temperature liquid slag, and the vapor film shrinks inward under external high pressure, so that the water comes into contact with the high temperature liquid slag, thereby generating water vapor. c and d indicate that at the moment when the water contacts the high-temperature liquid slag, a large amount of water vapor is locally generated, thereby generating a local high pressure, so that the surface of the high-temperature liquid slag forms a peak and extends outward. At this time, the high pressure rapidly discharges the water around the liquid residue, so that the active area rapidly expands.

The pictures e to h show that the peaks on the surface of the high-temperature liquid slag continuously grow, and breakage occurs, thereby forming liquid slag particles, and granulation occurs.

We simulate the shape of the local vapor film and wire produced by water vapor as shown below:

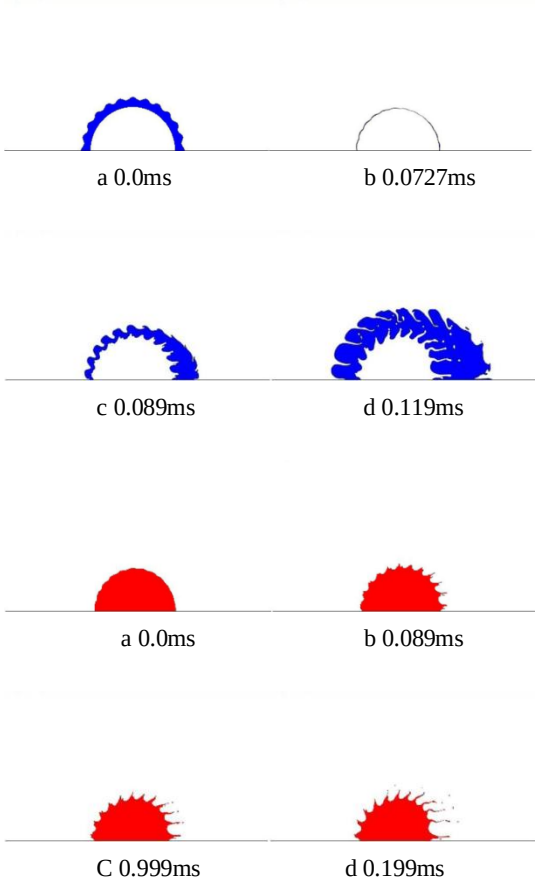

Fig.4.2 Vapor behavior and metal filaments growth

The red area in Figure 4.2 represents the high temperature liquid slag. At the initial moment, the molten high temperature liquid slag is round. After the vapor film collapses in Figure b, the surface of the high temperature slag forms an uneven pressure field, forcing the surface of the liquid slag to form a peak. The peaks gradually grow and eventually break. From the two pictures c and d, the peaks of the spikes first break during the growth process, which is the granulation mechanism of the high temperature liquid residue.

4.3.3 Simulation of surface velocity values of high temperature liquid slag in different time periods under laminar flow model

A simulation diagram of the surface velocity values of high temperature liquid slag at different time periods under the laminar flow model is shown in Figure 4.3:

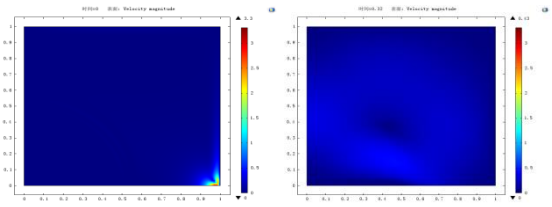

Fig.4.3 Surface velocity diagram of molten droplet at t=0-0.32s

Conclusion: It can be seen from the simulation diagram that when the high temperature liquid slag and water droplets have not met, the velocity of the high temperature liquid slag surface is relatively stable. However, when the high-temperature liquid slag comes into contact with water, the water vapor which is in contact with the water rapidly squeezes the liquid surface, thereby causing displacement of the liquid surface of the high-temperature liquid slag, thereby generating a speed.

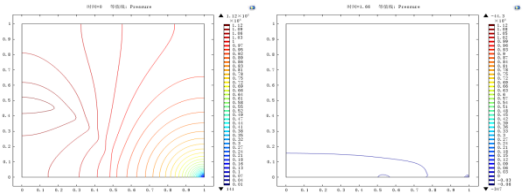

Fig.4.4 Contour map of t=0-1.66s molten drop pressure

The above figure shows the pressure distribution law of the high temperature liquid slag granulation process at different times. The external pressure triggers the transfer process. When the external force reaches 4.0 MPa, the high temperature liquid slag begins to granulate, but the pulse generated by the granulation process is much larger than the external force, so the high temperature liquid slag will produce small shock. The high temperature slag pressure contour follows the melting flow and solidification process, and the pressure at the same position during the flow is higher than the pressure at the solidification. That is, the pressure of the edge layer is greater than the pressure in the solid state when in a liquid state.

In this paper, the growth rate of high temperature liquid slag top filaments under different pressures and the transverse diameter of the interaction zone between high temperature liquid slag and water under different pressures are also calculated. as the picture shows:

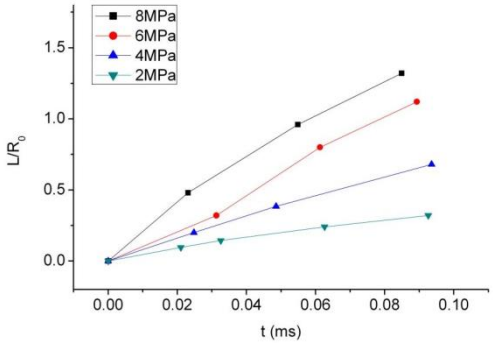

Fig.4.5 Filaments growth rate at the top of high temperature liquid slag under partial triggering pressure

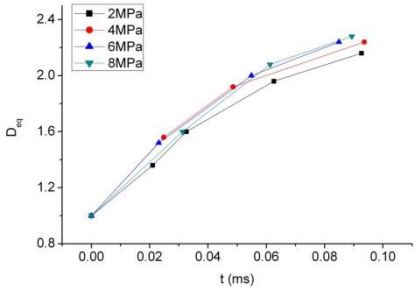

Fig.4.6 Transverse diameter of interaction zone between high temperature liquid slag and water under different triggering pressures

Figure 4-5 shows the filament growth rate curve at the top of the high-temperature liquid slag. In this paper, the growth rate of high temperature liquid slag top filaments under different pressures and the transverse diameter of the interaction zone between high temperature liquid slag and water under different pressures are also calculated. Figure 4-6 shows the transverse diameter of the interaction zone between water and high temperature liquid slag under different trigger pressures. It can be seen from the figure that the difference in the amount of steam generated is not large, so the impact of the contact area is not significant under different

triggering forces.

4.3.4 Simulation of surface temperature of high temperature liquid slag at different time periods under fluid heat transfer model

The first two figures below show the local reaction temperature field when the high temperature liquid slag is in contact with water, and the temperature isotherm in the middle.

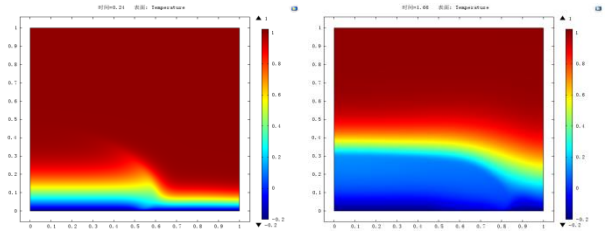

Fig. 4.7 Surface temperature diagram of molten drops at t=0-1.66s

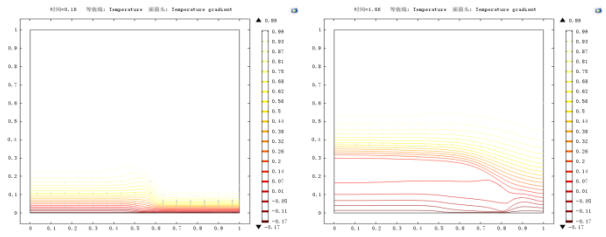

Fig. 4.8 Surface temperature gradient diagram of molten droplet at t=0.16-1.66s

Conclusion: It can be seen from the simulation diagram that the surface temperature gradient and the surface temperature map of the high temperature liquid slag are consistent, and the surface arrow is also oriented away from the outer surface, thereby verifying that the temperature away from the outer surface is getting higher and higher. It can be seen from the simulation diagram that the temperature of the surface temperature of the high temperature liquid slag is significantly lower than the temperature of the inner layer, and the farther away from the inner layer, the higher the temperature, and the farther away from the outer layer, the lower the temperature.

In addition, the paper also makes statistics on the growth rate of the top filament of the high temperature slag at different metal temperatures and the transverse diameter of the mutual region when interacting with water. The statistical graph is as follows.

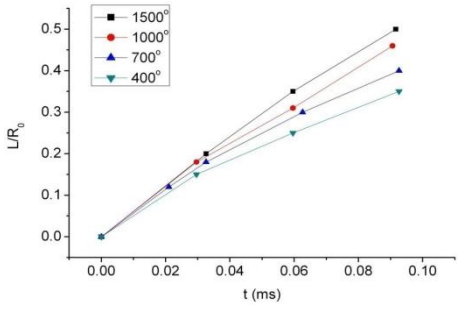

Fig.4-9 Growth rate of top filaments under different temperature conditions

Figure 4-9 shows that the growth rate of the filaments at the top of the high-temperature liquid slag increases as the temperature of the filament increases. The higher the metal temperature, the greater the amount of steam that is instantaneously generated upon contact with water, resulting in less uneven local pressure, As a result, the local pressure becomes more uneven, which increases the growth rate of filaments. Figure 4-10 shows the increase rate of the transverse diameter of the active area when the high temperature liquid slag interacts with water. Since the amount of steam generated at the moment of liquid-liquid contact increases, the expansion speed of the two-phase mixing action zone increases.

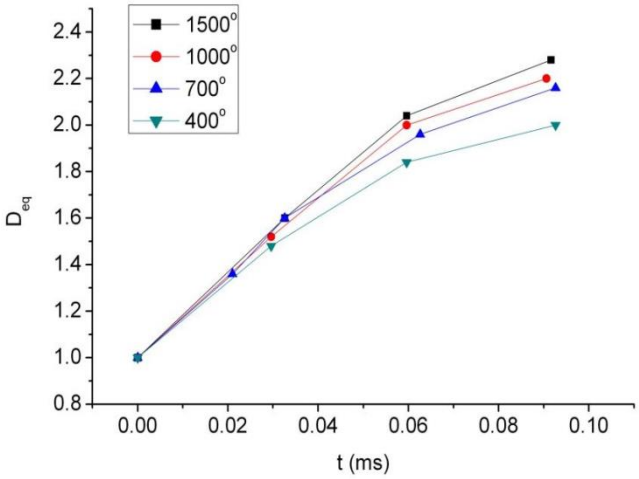

Fig.4-10 Variation of transverse diameter of interaction region under different temperatures

4.3.5 Comprehensive map of surface velocity, pressure and temperature of high temperature liquid slag in different time periods

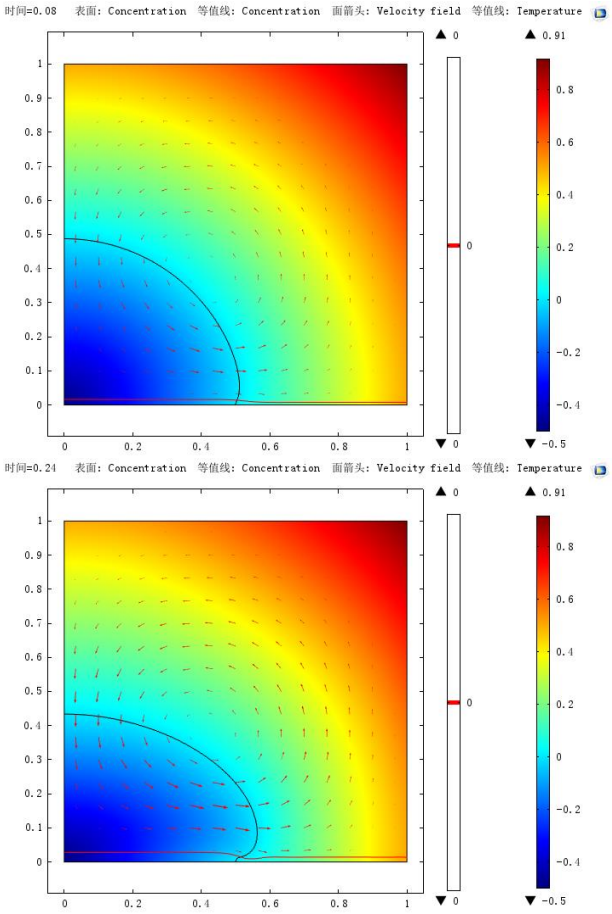

The above figure simulates the simulation results between four coupled physics fields in COMSOL, and the resulting legend results are basically similar to the actual situation. It can be explained that this method of simulation can not only simulate the reality realistically and quickly, but also provide a more convenient simulation method for scientific research.

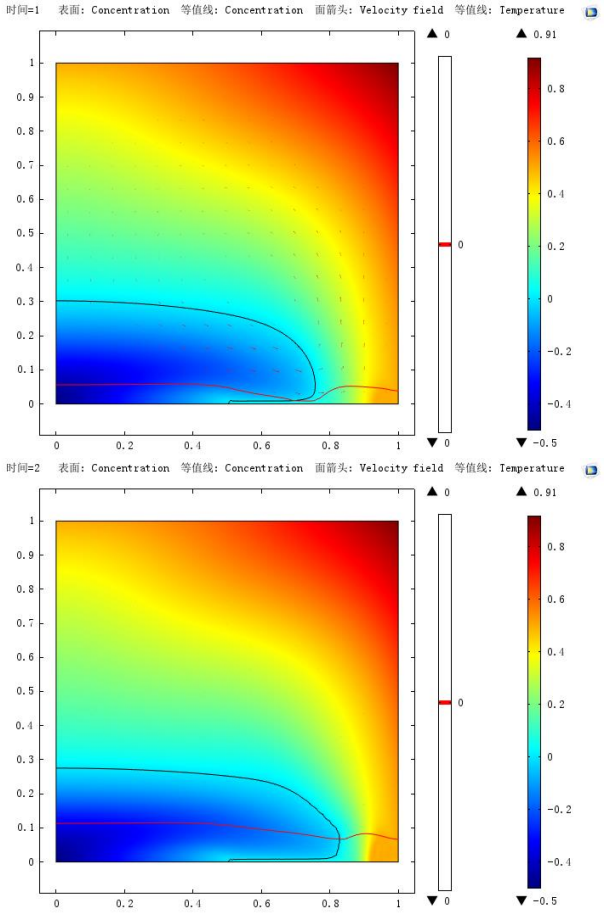

Fig. 4-11 Surface velocity, pressure and temperature of molten droplet

4.4 Simulated cloud image of the influence of different Laval nozzle diameters on the flow field

As can be seen from Fig. 4-12, as the Laval nozzle is continuously increased under certain conditions, the diameter of the core region of the jet formed by the high-temperature liquid slag crushing becomes larger and larger. It is known from the conservation theory that the speed of the broken high-temperature liquid slag is relatively smaller, but the broken area is getting larger and larger, so that the control binding force of the liquid slag is reduced, which indicates that the diameter of the Laval nozzle has a significant effect on the crushing of high temperature liquid slag. The effect of slag crushing is significant. The smaller the diameter of the Laval nozzle, the more the crushing zone will accumulate, the better the slag binding will be, and the better the speed parameters will be. However, production efficiency should be considered in actual production, so the diameter of the Laval nozzle cannot be infinitely small.

In addition to the above rules, it can be found that there is substantially no change in the fracture area before the nozzle diameter is D=14, when D=20, the diameter of the fracture zone increases sharply after the nozzle blows off the liquid slag, and the core fracture zone which is small with respect to the small diameter and the velocity almost disappears. Since the speed cannot be reached, the effect of crushing and granulating the high-temperature liquid slag is certainly not satisfactory. In summary, the optimum diameter of the Laval nozzle during high temperature liquid slag gas granulation should be 10 mm.

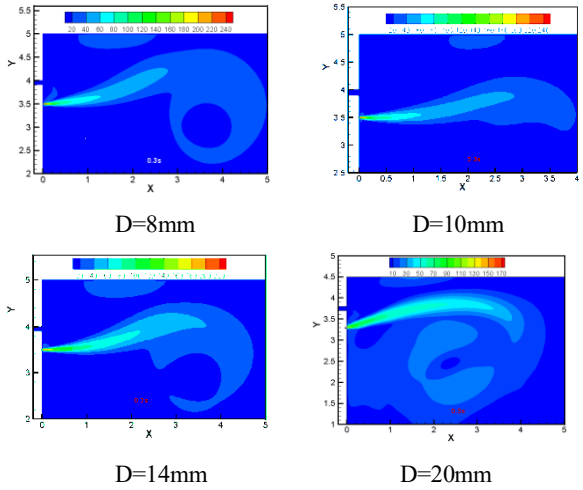

Fig.4-12 the flow field distribution of different nozzle diameter

4.5 Influence of Mach number of different fans on gas quenching and granulation

Figure 4-13, 4-14 below shows the velocity distribution of the indoor flow field during high temperature liquid slag gas quenching and granulation when the wind turbine power is 1.0 and 1.5 respectively. Through simulation study, it can be found that the length and width of the fracture area increase with the increase of the Mach number. In this way, the exchange of gas momentum and liquid slag momentum can be accelerated. Moreover, the Mach number has a great influence on the speed of the broken liquid slag. As the Mach number increases, the gas blowing speed increases significantly, which also makes the gas provide more impact kinetic energy per unit time. The high-temperature liquid slag is known by the law of conservation of momentum. The fragmentation naturally increases, which is obviously beneficial to the gas quenching and granulation process. In the same period of time, the fracture area of the high Mach number is relatively long due to the large velocity of the liquid slag.

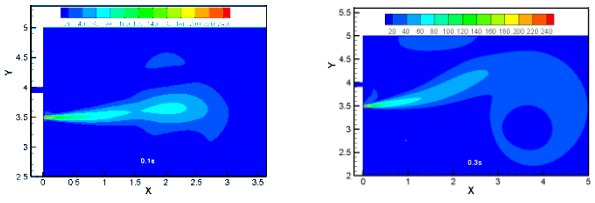

Fig.4-13 The flow field distribution of M=1.0

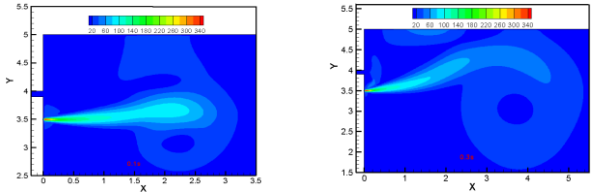

Fig.4-14 The flow field distribution of M=1.5

In addition, according to research and analysis, in the case of turbulent flow, the velocity decay law on the jet center line conforms to the following relationship

$$\frac{v_m}{v_0} = \frac{0.96}{\frac{ax}{r_0} + 0.29} \tag{38}$$

In the formula:

a —the experimental constant, equal to 0.07-0.08,

r_0 —the radius of the nozzle section,

v_m —jet central velocity,

v_0 —the initial speed of the exit

According to the analysis of Equation (38), under the same nozzle diameter, at the same position, the jet central velocity is proportional to the exit velocity, and the exit velocity is determined by the exit Mach number, that is, the larger the Mach number at the exit, the greater the jet central velocity.

5. Conclusion

The granulation process of high temperature liquid slag is a fairly complex process, because it involves heat transfer of fluid and the coupling of multiple physical fields and multiple phase transitions, so there are many factors affect the granulation process of high temperature liquid slag, such as temperature of high temperature liquid slag, surface tension of high temperature liquid slag, viscosity of high temperature liquid slag, external trigger force etc. The whole process can be divided into high temperature liquid slag granulation process and slag particle solidification process. In this paper, the fluid mechanics software COMSOL is used to simulate and calculate the granulation and solidification process of high temperature liquid slag to make statistics Icon, especially the growth rate of surface filaments and the expansion diameter of the area of contact between water and high temperature liquid slag. Some laws in the granulation process were revealed, such as the law of multi-field coupling of the pressure field, the distribution law of slag grain solidification temperature field, granulated surface and steam film of instant contact. These laws are in multi-field coupling of the pressure field, temperature field, velocity field and fluid mechanics field in the granulation process and provide theoretical support and visualization results for granulation and heat recovery.

The most important thing in this paper is to use the SIMPLE algorithm of staggered grid to develop a multidimensional coordinate system to represent the calculation steps of multiple phase fluid heat transfer, which provides a mathematical basis for studying such problems. Firstly, the process of water-quenching treatment of high-temperature liquid slag is mainly simulated, and the simulation results are basically consistent with the actual experimental results. The calculation results show that the intense heat transfer and the filament growth crack on the surface of the high temperature liquid slag are the main reasons for the granulation of the high temperature liquid slag. And in which the intense heat transfer is caused by the instant contact between the water droplets. Secondly, the simulation of the morphology of the contact filament, the shape of the vapor film, the temperature, and the pressure and the velocity of the high temperature liquid slag surface were made.

The simulation was carried out under the action of external triggering force, which indicated that the growth and fracture of metal filament on the surface of high temperature liquid slag is the main reason for granulation. In addition, the growth rate of the filament is proportional to the external pressure and the temperature of the high temperature liquid slag. However, the external force has little effect on the expansion speed of the reaction zone. On the contrary, the self-temperature of the liquid slag has a great influence on the surrounding physical field and the expansion speed of the reaction area.

The diameter of the Laval nozzle is increased, the length of the core of the jet is increased, the speed is reduced, the width of the gas jet is increased, and the bundling property of the jet becomes poor. The diameter of the Laval nozzle is too small, and the reduction of the diameter of the nozzle increases the fluid. Resistance, on the other hand, requires more motor power at the same gas flow rate. Taken together, the optimum diameter of the Laval nozzle is D = 10mm. The Mach number of the jet, within the allowable range, is more favorable for the granulation of the slag particles.

Aiming at the research work of this paper, the physical mechanism of high temperature liquid slag in the process of crushing and granulation is summarized, and the research ideas in related fields are provided. It has certain inspiration and practical value for the related research work.

References

[1] Guang Chen, Hengda Wang, Xiangjun Bao, et al. A blast furnace slag dry treatment method based on high temperature slag waste heat recovery: CN106521056A[P]. 2017.

[2] Yonghui Wang, Haifeng Chang, Taiqiang Sun , et al. Reform practice of water quenching slag in smelting furnace[J]. Hunan Nonferrous Metals, 2018(1).

[3] Sheng Qi. Problems and Solutions in the Application of Thermal Energy and Power Engineering in Boiler[J]. Science and Technology Innovation and Application, 2014(17): 109-109.

[4] Qihua Huang. Application of finite element method in analysis of underground transient temperature field of soil source heat pump[D]. North China University of Technology, 2010.

[5] Ban G, Dai J. Analysis of Single Layer Coverage Governance Effects of Uranium Tailings Pile Based on COMSOL Software[J]. Modern Mining, 2018.

[6] Monjezi S, Palaniappan M B, Jones J D, et al. Dynamic Simulation of a Polymer Molecule Using COMSOL Multiphysics: DNA Separation in a Microchannel[C]// COMSOL Conference. 2017.

[7] Miaohong Yan. Numerical simulation of solidification process of blast furnace slag particles [D]. Northeastern University, 2007.

[8] Yunhua Zhang, Meicheng Yan, Changsong Chen. Numerical calculation methods and algorithms [M]. Science Press, 2000.

[9] Wen Jia. “Stability Theory of Ordinary Differential Equations”[J]. Chinese Science Bulletin, 1962(8): 51.

[10] Hong Xu, Xiuchen Yang, Wei Gu, et al. Overview of measurement and calculation methods for mold/sheet interface contact thermal resistance during hot forming and quenching process[J]. Forging & Stamping Technology, 2015, 40(5): 124-129.

[11] Turgay M B, Yazıcıoğlu A G. Numerical simulation of fluid flow and heat transfer in a trapezoidal microchannel with COMSOL multiphysics: A case study[J]. Numerical Heat Transfer Part A - Applications, 2018, 73(5):1-15.

[12] Menshykau D, Adivarahan S, Germann P, et al. Simulating Organogenesis in COMSOL: Parameter Optimization for PDE-based models[J]. 2011.

[13] Lianggui Peng, Ming Yu, Zhaodong Wang, et al. A Review of Mathematical Models for Laminar Cooling of Hot Rolled Strip[J]. Rolled Steel, 2003, 20(6): 25-29.

[14] Jinsheng Xiao, Bingcheng Deng, Changming Yu. Variational Principles and Generalized Variational Principles for Heat Conduction Problems[J]. Applied Mathematics, 1988(4): 103-109.

[15] JU Brackbill. FLIP MHD - A particle-in-cell method for magneto hydrodynamics[J]. Journal of Computational Physics, 1990, 91(2):497-497.

[16] Guozhi Zhao, Fanrang Kong, Jingchun Zhan, et al. Numerical Simulation of Turbulent Flow Field Based on SIMPLE Algorithm[J]. Hydroelectric Energy Science, 2007, 25(3): 100-102.

[17] Wu W, Hu C, Hu J, et al. Jet cooling characteristics for ball bearings using the VOF multiphase model[J]. International Journal of Thermal Sciences, 2017, 116:150-158.

[18] Saha D, Mirando N, Levchenko A. Liquid and vapor phase adsorption of BTX in lignin derived activated carbon: Equilibrium and kinetics study[J]. Journal of Cleaner Production, 2018, 182.
[19] FengXian Sun, Jin Yang, ChangYu Liu, et.. Surface Tension Effect of Droplet Evaporation in High Temperature Gas Flow[J]. Journal of Engineering Thermophysics, 2016, V37(1): 176-179.
[20] Weiping Qu, Jiang Song, Yongfeng Liang, et al. Phase field simulation of superalloys for advanced aviation turbine engines [English] [C]// System simulation technology and its applications. 2015.
[21] [21] Cahn–Hilliard equation[J]. Applicable Analysis, 2013, 92(5):1028-1045.
[22] Galdi G P. An Introduction to the Mathematical Theory of the Navier-Stokes Equations[M]. Springer New York, 2011.
[23] Shuzhong Wang , Hong Zhang, Wei Zhao, et al. A skid-mounted supercritical pressure DC steam injection boiler: CN101144612[P]. 2008.
[24] Yager P, Brody J P. Laminar flow: US, US 5971158 A[P]. 1999.
[25] Tan Jia-wei, The Mechanical Meaning of Bernstein Basis Function. International Journal of Applied Mathematics in Control Engineering, 2018. 1(1): p. 47-54.
[26] W. Wei, Liang B., and Zuo M., Linear Active Disturbance Rejection Control for Nanopositioning System. International Journal of Applied Mathematics in Control Engineering, 2018. 1(1): p. 92-95.
[27] W.J. Wu, Parametric Lyapunov Equation Approach to Stabilization and Set Invariance Conditions of Linear Systems with Input Saturation. International Journal of Applied Mathematics in Control Engineering, 2018. 1(1): p. 79-84.
[28] T. Zhao and Wang J., Multimodal Transport Path Planning based on Multilateration (MLAT) System Using a Pulse Neural Network Model. International Journal of Applied Mathematics in Control Engineering, 2018. 1(1): p. 55-61.

Jincai Chang received his B.Sc. degree in 1996 from Ocean University of China ，received his M. Sc. degree in 2005 from Yanshan University ，received his Ph.D. degree in 2008 from Dalian University of technology, now he is Professor in North China University of Science and technology. His main research interests include theories and methods in mathematical modelling and scientific computation, numerical approximation and computational geometry, etc.

Yafei Zhu received a Bachelor's degree in applied mathematics from Hebei North University and is now a graduate student in computational mathematics in North China University of Science and Technology. In the past four years, she has taken several specialized courses, including mathematical analysis and numerical analysis. Her research fields include radial basis function neural network, B spline.

QiulingPan received a Bachelor's degree in information and computation science from Hebei North University and is now a graduate student in computational mathematics in North China University of Science and Technology. Her research fields include theories and methods in numerical approximation and B spline.

Xing Xin graduated from north China university of science and technology with a major in information and computing science in 2018.During my college years, I have been following professor chang jincai to study the problem of multiple physical field coupling.Won the first prize of American mathematical modeling contest and many other mathematical modeling awards.